UV-Induced Coupling of 4-Vinylbenzyl Chloride on Hydrogen-Terminated Si(100) Surfaces for the Preparation of Well-Defined Polymer−Si Hybrids via Surface-Initiated ATRP

F. J. Xu, E. T. Kang,* and K. G. Neoh

Department of Chemical and Biomolecular Engineering, National University of Singapore, Kent Ridge, Singapore 119260

Received April 21, 2004; Revised Manuscript Received December 9, 2004

ABSTRACT: The simple approach of UV-induced coupling of 4-vinylbenzyl chloride (VBC) with the hydrogen-terminated Si(100) (the Si−H) surface provided a stable Si−C bonded initiator monolayer (the Si−VBC surface) for the surface-initiated atom transfer radical polymerization (ATRP). Well-defined polymer−Si hybrids, consisting of covalently tethered polymer brushes of sodium 4-styrenesulfonate (NaStS) and poly(ethylene glycol) monomethacrylate (PEGMA) on single crystal silicon substrates, were prepared. Kinetic studies revealed an approximately linear increase in both graft polymer concentration and polymer film thickness with the polymerization time, indicating that the chain growth from the functionalized silicon surface was a controlled process with a "living" character. Atomic force microscopy (AFM) images suggested that the surface-initiated ATRP had proceeded uniformly on the Si−VBC surface to give rise to a dense and molecularly flat surface coverage. The "living" chain ends were used as the macroinitiator for the synthesis of diblock copolymer brushes, consisting of the NaStS polymer (P(NaStS)) and the PEGMA polymer (P(PEGMA)) blocks.

1. Introduction

Tethering of polymer brushes on a solid substrate is an effective method of modifying the surface properties of the substrate.[1,2] Recently, considerable attention has been paid to the manipulation and control of the physicochemical properties of single-crystal silicon surfaces because of their crucial importance to the modern microelectronics industry.[2−7] In many cases, the dense polymer brushes can serve as an effective etching barrier in the microlithographic process, provide excellent mechanical and chemical protection of the substrate, alter the electrochemical interface characteristics of the substrate, and provide new pathways to the functionalization of silicon surfaces for molecular recognition and sensing.[8−11]

The synthesis of polymers with well-defined compositions, architectures, and functionalities has long been of great interest in polymer chemistry. With the progress in polymerization methods, it is possible to prepare well-defined graft polymer chains on various substrate surfaces by cationic polymerization,[12] anionic polymerization,[13] radical polymerization,[14] nitroxide-mediated radical polymerization,[15] reversible addition−fragmentation chain transfer polymerization,[16] and atom transfer radical polymerization (ATRP).[17−19] ATRP is a recently developed "living" radical polymerization method, involving a copper halide/nitrogen-based ligand catalyst.[20] The method does not require stringent experimental conditions, as in the case of cationic and anionic polymerization. This controlled radical polymerization technique allows for the polymerization and block copolymerization of a wide range of functional monomers, such as styrene,[21,22] acrylates,[23] and methacrylates[24] in a controlled fashion, yielding polymers with narrowly dispersed molecular weights, predetermined by the concentration ratio of the consumed monomer to initiator.[25] There are a number of reports in the literature dealing with the modification of silicon surfaces by ATRP.[6,26−33] Surface initiators were immobilized on the oxidized silicon surface, the hydrogen-terminated silicon surface, or the monolayer-modified silicon wafer, usually in multistep processes.

In this work, we report on an alternative one-step approach to the covalent attachment (Si−C bonding) of an ATRP initiator on the oriented single-crystal silicon surface via UV-induced coupling of 4-vinylbenzyl chloride (VBC) with the hydrogen-terminated Si(100) surface (Si−H surface). Polymer brushes of sodium 4-styrenesulfonate (NaStS) and poly(ethylene glycol) (PEGMA), and diblock copolymer brushes of NaStS and PEGMA, were prepared via surface-initiated ATRP on the VBC-coupled silicon (Si−VBC) surface to give rise to the well-defined polymer−Si hybrids. The chemical composition and topography of the modified silicon surfaces were characterized by X-ray photoelectron spectroscopy (XPS) and atomic force spectroscopy (AFM), respectively.

2. Experimental Section

2.1. Surface Characterization. The chemical composition of the modified silicon surfaces was determined by X-ray photoelectron spectroscopy (XPS). The XPS measurements were performed on a Kratos AXIS HSi spectrometer using a monochromatized Al Kα X-ray source (1486.6 eV photons) at a constant dwell time of 100 ms and a pass energy of 40 eV. The samples were mounted on the standard sample studs by means of double-sided adhesive tapes. The core-level signals were obtained at a photoelectron takeoff angle (α, measured with respect to the sample surface) of 90°. The X-ray source was run at a reduced power of 150 W (15 kV and 10 mA). The pressure in the analysis chamber was maintained at 10^{-8} Torr or lower during each measurement. All binding energies (BE's) were referenced to the C 1s hydrocarbon peak at 284.6 eV. In peak synthesis, the line width (full width at half-maximum, or fwhm) for the Gaussian peaks was maintained constant for all components in a particular spectrum. Surface elemental

* To whom all correspondence should be addressed: Tel +65-6874-2189; Fax +65-6779-1936; e-mail cheket@nus.edu.sg.

10.1021/ma049225a CCC: $30.25
Published on Web 02/03/2005

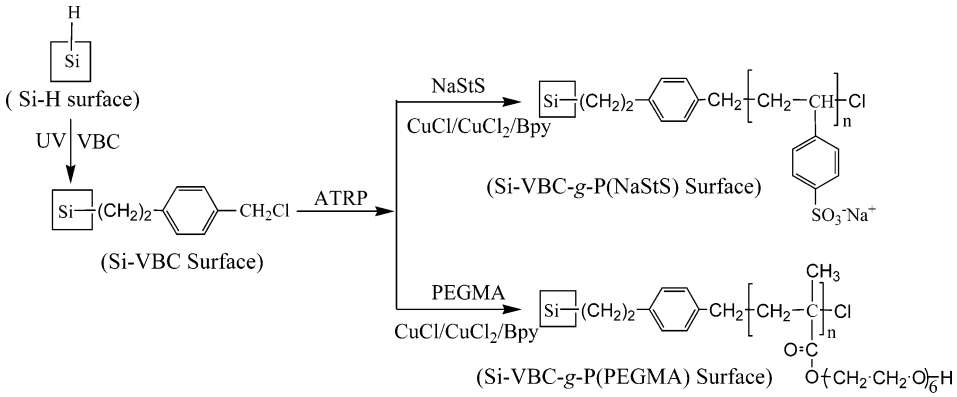

Figure 1. Schematic diagram illustrating the processes of UV-induced coupling of VBC on the Si−H surface to give the Si−VBC surface and the Si−VBC surface-initiated ATRP of NaStS and PEGMA.

stoichiometries were determined from XPS spectral area ratios and were reliable to within ±5%. The elemental sensitivity factors were calibrated using stable binary compounds of well-established stoichiometries.

The static water contact angles of the pristine and functionalized Si−H surfaces were measured at 25 °C and 60% relative humidity, using the sessile drop method with a 3 μL water droplet, in a telescopic goniometer (Rame-Hart model 100-00-(230), manufactured by the Rame-Hart, Inc., Mountain Lakes, NJ). The telescope with a magnification power of 23× was equipped with a protractor of 1° graduation. For each angle reported, at least three measurements from different surface locations were averaged. The angle reported was accurate to ±3°.

The thickness of the polymer brushes grafted on the silicon substrate was determined by ellipsometry. The measurements were carried out on a variable angle spectroscopic ellipsometer (model VASE, J.A. Woollam Inc., Lincoln, NE) at incident angles of 70° and 75° in the wavelength range 200−1000 nm. Organic films typically have indices of refraction in the range of 1.4−1.5.[34] In this work, the refractive indices of the NaStS and PEGMA polymers were taken to be 1.45 in the Cauchy film model used for the simulation of film thickness. For each sample, the thickness measurements were made on at least four different surface locations. Data were recorded and processed using the WVASE32 software package.

The topography of the modified silicon surfaces was studied by atomic force microscopy (AFM), using a Nanoscope IIIa AFM from the Digital Instrument Inc. In each case, an area of 5 × 5 μm^2 was scanned using the tapping mode. The drive frequency of the equipment, with the voltage between 3 and 4.0 V, was 330 ± 50 kHz. The drive amplitude was about 300 mV, and the scan rate was 0.5−1.0 Hz. The arithmetic mean of the surface roughness (R_a) reported was calculated from the roughness profile determined by AFM.

2.2. Materials. (100)-oriented single crystal silicon, or Si-(100) wafers, with a thickness of about 1.5 mm and a diameter of 150 mm, were purchased from Unisil Co. of Santa Clara, CA. The as-received wafers were polished on one side and doped lightly as n-type. The silicon wafers were sliced into square chips of about 1.2 cm × 1.2 cm in size. To remove the organic residues on the surface, the silicon substrate was washed with the "piranha" solution, consisting of 98 wt % concentrated sulfuric acid (70 vol %) and hydrogen peroxide (30 vol %). After rinsing with copious amounts of doubly distilled water, the silicon chips were dried at 70 °C in a vacuum oven for 2 h.

Hydrofluoric acid (HF) (37 wt %), 4-vinylbenzyl chloride (VBC, 97%), 2,2′-byridine (Bpy, 99%), copper(I) chloride (99%), copper(II) chloride (97%), and poly(ethylene glycol) monomethacrylate (PEGMA) macromonomer ($M_n \sim$ 360 g/mol, liquid, >99%) were obtained from Aldrich Chemical Co. of Milwaukee, WI. The monomer used for graft copolymerization, sodium 4-styrenesulfonate (NaStS, MW ~206 g/mol, powder, >99%), was obtained from Wako Pure Chemical Industries Ltd. of Tokyo, Japan. PEGMA was passed through the silica gel column to remove the inhibitor and stored in an argon atmosphere at −10 °C.

2.3. Immobilization of the Initiator on the Si−H Surface. The pristine (oxide-covered) silicon chips of about 1.2 cm × 1.2 cm in size were immersed in 20 mL 10 vol % HF in individual Teflon vials for 2 min to remove the oxide film and to leave behind a uniform H-terminated Si(100) surface (the Si−H surface).[3,7,29,35] The initiators were immobilized via UV-induced coupling of VBC with the Si−H surface to give rise to a covalently bonded (Si−C bonded) monolayer (the Si−VBC surface). The process is shown schematically in Figure 1.

For the UV-induced coupling of VBC with the Si−H surface, about 0.2 mL of the VBC was introduced onto the freshly prepared Si−H surface of about 1.2 cm × 1.2 cm in size. The Si−H chip was sandwiched between two quartz plates of 1.5 cm × 4.0 cm in size, and a uniform thin liquid film of VBC formed on the Si−H surface. The assembly was placed in a Pyrex tube of 2 cm in diameter and subjected to UV irradiation for 3 min in a Riko RH400-10W rotary photochemical reactor (manufactured by Riko Denki Kogyo of Chiba, Japan). The reactor was equipped with a 1000 W high-pressure Hg lamp and a constant-temperature bath. All UV-induced reactions were carried out at a constant temperature of 28 °C. After UV irradiation, the silicon substrate was washed thoroughly in an excess amount (about 200 mL) of acetone, a good solvent for VBC and its polymer, for 24 h, followed by rinsing with copious amounts of fresh acetone. The VBC-coupled Si−H (Si−VBC) substrate was then dried by pumping under reduced pressure. Surface composition calcd for VBC: [Cl]/[C] = 1.0/9.0. Found from XPS analysis: [Cl]/[C] = 0.98/9.0. Surface water contact angle: 86°. A control experiment, in which the Si−H substrate was soaked in neat VBC for the same period of time, but in the absence of UV irradiation, was also carried out. No VBC molecules were detected on the Si−H surface after the substrate was rinsed briefly with acetone and subjected to surface analysis by XPS.

2.4. Surface-Initiated Atom Transfer Radical Polymerization (ATRP). For the preparation of the NaStS polymer (P(NaStS)) brushes on the Si−VBC surface, NaStS (1.0 g, 4.8 mmol), CuCl (4.85 mg, 0.048 mmol), $CuCl_2$ (1.29 mg, 0.0096 mmol), and Bpy ligand (15 mg, 0.096 mmol) were added to 5 mL of doubly distilled water in a Pyrex tube. The mixture was stirred and degassed with argon for 30 min. The Si−VBC substrate (about 1.2 cm × 1.2 cm in size) was then introduced into the reaction mixture. The reaction tube was sealed and kept in a 30 °C water bath for 0.5−3 h. After the reaction, the silicon substrate with surface grafted P(NaStS) (the Si−VBC-*g*-P(NaStS) surface) was removed from the reaction mixture and washed thoroughly with continuous stirring in about 200 mL of doubly distilled water for 24 h. It was subsequently rinsed with about 100 mL of doubly distilled water. The substrate was dried for 10 h by pumping under reduced pressure. P(NaStS) film thickness after 3 h of ATRP: 7 nm. Surface composition calcd for P(NaStS): [S]/[Na] = 1.0. Found from XPS analysis: [S]/[Na] = 1.2. Surface water

contact angle: 29°.

For the preparation of PEGMA polymer (P(PEGMA)) brushes on the Si−VBC surface, PEGMA (0.80 mL, 2.4 mmol), CuCl (2.38 mg, 0.024 mmol), $CuCl_2$ (0.65 mg, 0.005 mmol), and Bpy ligand (7.5 mg, 0.05 mmol) were added to 5 mL of doubly distilled water in a Pyrex tube. The mixture was stirred and degassed with argon for 30 min. The Si−VBC substrate (about 1.2 cm × 1.2 cm in size) was introduced into the reaction mixture. The reaction tube was sealed and kept in a 30 °C water bath for 0.5−3 h. After the reaction, the silicon substrate with surface grafted P(PEGMA) (the Si−VBC-*g*-P(PEGMA) surface) was removed from the solution and washed thoroughly with an excess amount of doubly distilled water, following the same procedures as those described above for the Si−VBC-*g*-P(NaStS) surface. The substrate was dried by pumping under reduced pressure. P(PEGMA) film thickness after 3 h of ATRP: 8 nm. Surface composition calcd for P(PEGMA): [C−O]/[O=C−O] = 12. Found from XPS analysis: [C−O]/[O=C−O] = 10.5. Surface water contact angle: 43°.

One of the unique characteristics of the polymers synthesized by ATRP is the preservation of the active or "living" end groups throughout the polymerization reaction. To confirm the presence of active chain ends in the grafted NaStS (or PEGMA) polymer, diblock copolymer brushes consisting of P(NaStS) and P(PEGMA) blocks were prepared by using the P(NaStS) (or P(PEGMA)) brushes on the Si−VBC surface (Figure 1) as the macroinitiators for the ATRP of the second monomer PEGMA or NaStS. For the preparation of the P(NaStS)-*b*-P(PEGMA) copolymer brushes on the Si−VBC-*g*-P(NaStS) surface (or the P(PEGMA)-*b*-P(NaStS) copolymer brushes on the Si−VBC-*g*-P(PEGMA) surface), the Si−VBC-*g*-P(NaStS) substrate (or the Si−VBC-*g*-P(PEGMA) substrate) was used instead of the Si−VBC substrates under the same reaction conditions as described above for the preparation of the initial homopolymer block.

3. Results and Discussion

3.1. Immobilization of the Initiator on the Si−H Surface. The chemical composition of the silicon surfaces at various stages of surface modification was determined by XPS. Two peak components at the binding energies (BE's) of about 99 and 103 eV, attributable to the *Si*−Si and *Si*−O species, respectively,[29] are observed in the XPS Si 2p core-level spectrum of the pristine (oxide-covered) silicon surface (Figure 2a). To obtain the hydrogen-terminated silicon (Si−H) surface, the pristine silicon chip (Si(100) substrate) was treated with dilute hydrofluoric acid solution to remove the native oxide layer.[3,7,29,35] No oxidized silicon species in the BE region of 101−103 eV was detected in the Si 2p spectrum after the HF treatment (Figure 2b). This result is consistent with the formation of a predominantly hydrogen-terminated silicon surface.[3,7,29,35]

For the preparation of polymer brushes on the silicon surface, a uniform and dense monolayer of initiators immobilized on the silicon surface is indispensable. The initiators are immobilized via UV-induced coupling of VBC on the Si−H surface to give rise to a stable initiator monolayer via the Si−C bonds. The Si−H group on the Si−H surface can be homolytically dissociated by UV irradiation to form a radical site, which reacts readily with an alkene to give rise to a surface-tethered alkyl radical on the β-carbon. The radical subsequently abstracts an H atom from the adjacent Si−H bond. The abstraction creates a new reactive silicon radical to allow the above reaction to propagate as a chain reaction on the Si−H surface.[3,7,35,36] Figure 2c,d shows the corresponding C 1s and Cl 2p core-level spectra of the VBC coupled Si−H surface (Si−VBC surface). The C 1s core-level spectrum of the Si−VBC surface can be curve-fitted into three peak components having BE's at about

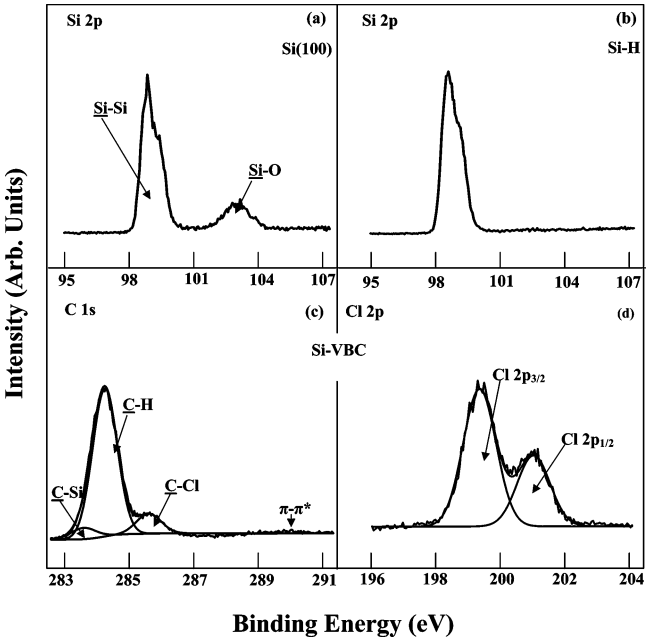

Figure 2. Si 2p core-level spectra of (a) the pristine (oxide-covered) Si(100) and (b) the Si−H surface and (c) C 1s and (d) Cl 2p core-level spectra of the Si−VBC surface.

283.9, 284.6, and 286.2 eV, attributable to the *C*−Si species, *C*−H species, and *C*−Cl species, respectively.[37,38] The presence of the *C*−Si peak component in the C 1s spectrum is unambiguous. UV-induced formation of a very stable Si−C bond between the Si−H surface and alkyl monolayer has been well-established.[3,7,35,36] The $\pi-\pi^*$ shake-up satellite of the benzyl group of VBC is also discernible at the BE of about 290.4 eV. The Cl 2p core-level spectrum in Figure 2d consists of the Cl $2p_{3/2}$ and Cl $2p_{1/2}$ peak components at the BE's of about 199.3 and 201.5 eV, respectively, attributable to the covalently bonded chlorine species. The appearance of the *C*−Si and *C*−Cl species, as well as the $\pi-\pi^*$ shake-up satellite, confirms the presence of a reactively coupled VBC layer on the Si−H surface. Thus, the benzyl chloride groups have been successfully immobilized on the Si−H surface to cater for the subsequent ATRP process on the Si−VBC surface. The fact that the [*C*−Cl]/[*C*−H] component area ratio (∼0.13) in Figure 2c is very close to the theoretical ratio of 0.125 for the VBC molecule suggests that UV-induced formation of benzyl radical probably has not occurred to a significant extent. A substantial increase in water contact angle of the Si−VBC surface, from that of the Si−H surface (Table 1), is consistent with the complete coverage of the Si−H surface by VBC. The complete coverage, however, probably does not mean complete replacement of Si−H by Si−C bonds. Experiment and theoretical studies have suggested that a maximum of about 60% of the hydrogen sites on the hydrogen-terminated Si(100) are substituted by alkyl group at complete surface coverage.[35]

3.2. Si−VBC Surface-Initiated ATRP. The physicochemical properties of the silicon surface can be tuned by the choice of a variety of vinyl monomers. In this work, two functional monomers, sodium 4-styrenesulfonate (NaStS) and poly(ethylene glycol) monomethacrylate (PEGMA), were selected as the model monomers. NaStS is a commercially important anionic monomer with a wide range of applications, ranging from fuel cell to humidity sensor.[39,40] The NaStS polymer (P(NaStS)),

Table 1. Chemical Composition, Static Water Contact Angle, and Layer Thickness of the Graft Polymerization Silicon Surfaces

sample	[S]:[Na][a]	[C−O]:[O=C−O][a]	static water contact angle (±3°)[b]	layer thickness (±1 nm)[c]
Si−VBC-*g*-P(NaStS) surface[d]	1.2:1(1:1)	0:0:0 (0:0)	29	7
Si−VBC-*g*-P(PEGMA) surface[e]	0:0 (0:0)	12:1 (10.5:1)	43	8

[a] Determined from the XPS core-level spectra area ratio. Values in parentheses are the theoretical ratio. [b] Static water contact angles for the pristine (oxide-covered) Si(100) surace, the Si−H surface, and the Si−VBC surface are about 20°, 72°, and 86°, respectively. [c] The thickness of the VBC monolayer on the Si−VBC surface is about 0.3 nm. [d] Reaction conditions: [NaStS]:[CuCl]:[$CuCl_2$]:[Bpy] = 100:1:0.2:2, temperature 30 °C, reaction time 3 h. [e] Reaction conditions: [PEGMA]:[CuCl]:[$CuCl_2$]:[Bpy] = 100:1:0.2:2, temperature 30 °C, reaction time 3 h.

with both hydrophilic and hydrophobic groups, possesses an amphiphilic character. The physicochemical properties are strongly affected by the sequence of the sulfonic acid groups and the molecular weight distribution of the polymer.[41] The hydroxyl end groups of the grafted PEGMA polymer (P(PEGMA)) side chains could be converted into various functional derivatives.[42] In addition, the P(PEGMA)-grafted silicon surface is effective in preventing protein adsorption and platelet adhesion.[43]

At the beginning stage of ATRP, a sufficient concentration of the deactivating Cu(II) complex is necessary to quickly establish an equilibrium between the dormant and the active chains. If this equilibrium is not controlled properly, the process resembles that of the conventional redox-initiated radical polymerization.[44] The Cu(II) complex can be obtained by the reaction of Cu(I) complex with the initiator or by addition of the complex at the begin of reaction.[45] In this work, the method of addition of the Cu(II) complex ($CuCl_2$) was chosen to control the surface-initiated ATRP of NaStS or PEGMA on the Si−VBC surface. The ratio of [NaStS or PEGMA (monomer)]:[CuCl (catalyst)]:[$CuCl_2$ (deactivator)]:[Bpy (ligand)] is controlled at 100:1:0.2:2.

The presence of grafted P(NaStS) (or P(PEGMA)) on the Si−VBC surface was confirmed by XPS analysis. Figure 3a,b shows the respective S 2p and Na 1s core-level spectra of the Si−VBC-*g*-P(NaStS) surface of 3 h of ATRP. The S 2p spectrum consists of the S $2p_{3/2}$ and S $2p_{1/2}$ peak components of the sulfonate species at the BE's of about 163.8 and 165 eV, respectively.[46] On the other hand, the Na 1s core-level spectrum appears at the BE of about 1068.5 eV.[47] The presence of the S 2p and Na 1s species indicates that P(NaStS) has been successfully grafted on the Si−VBC surface via ATRP. The C 1s core-level spectrum of the as-prepared Si−VBC-*g*-P(PEGMA) surface is shown in Figure 3c. The C 1s core-level spectrum can be curve-fitted into three peak components with BE's at about 284.6, 286.2, and 288.5 eV, attributable to the *C*−H, the *C*−O, and the O=*C*−O species, respectively.[37,38] The appearance of the two prominent peak components, assigned to the *C*−O and O=*C*−O species of PEGMA, confirms that P(PEGMA) has been successfully grafted on the Si−VBC surface. The S 2p and Na 1s core-level spectral line shapes of the Si−VBC-*g*-P(NaStS) surface and the C 1s core-level spectral line shape of the Si−VBC-*g*-P(PEGMA) surface remain practically unchanged throughout the ATRP process. In addition, the [S]/[Na] and [C−O]/[O=C−O] ratios, obtained by XPS, are also in fairly good agreement with their respective theoretical ratios (Table 1) throughout the course of ATRP.

As shown in Table 1, the variation in static water contact angles for the functionalized silicon surfaces suggests that the hydrophilicity of the silicon surfaces can be readily tuned. The static water contact angle of the pristine (oxide-covered) Si(100) surface is about 20°.

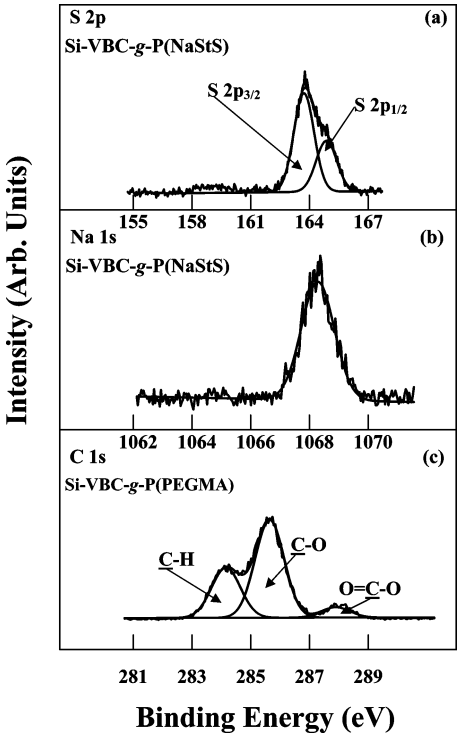

Figure 3. (a) S 2p and (b) Na 1s core-level spectra of the Si−VBC-*g*-P(NaStS) surface (reaction conditions: [NaStS]:[CuCl]:[$CuCl_2$]:[Bpy] = 100:1:0.2:2, temperature = 30 °C, reaction time = 3 h) and (c) C 1s core-level spectrum of the Si−VBC-*g*-P(PEGMA) surface (reaction conditions: [PEGMA]:[CuCl]:[$CuCl_2$]:[Bpy] = 100:1:0.2:2, temperature = 30 °C, reaction time = 3 h).

The water contact angles for the Si−H surface and the Si−VBC surface are about 72° and 86°, respectively. When the silicon surface was grafted with a P(NaStS) layer, the water contact angle decreases to about 29°. When grafted with a P(PEGMA) layer, the silicon surface becomes less hydrophilic, and the contact angle increases to about 43°.

The kinetics of P(NaStS) growth from the Si−VBC surface via ATRP was investigated. In a typical XPS spectral measurement, the spectral signal intensities come from a fixed sampling depth at a particular photoelectron takeoff angle (α).[48] For the Si−VBC-*g*-P(NaStS) surface, the overall signals of the graft and the substrate are represented by the S 2p core-level spectrum from the P(NaSt) layer and the Si 2p core-level spectrum from the underlying silicon substrate, all within the sampling depth of about 7.5 nm (α = 90°).[29,49] As shown by line a in Figure 4, there is an approximately linear relationship between the P(NaStS) graft concentration, expressed as the [S]/([S] + [Si]) ratio (([S] + [Si]) is the sum of the sensitivity factor-corrected

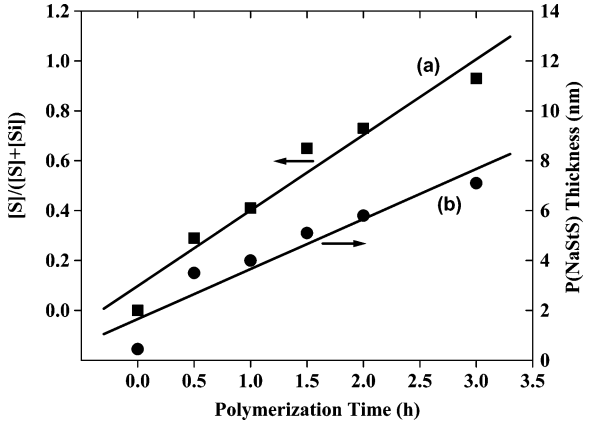

Figure 4. Dependences of (a) the overall graft concentration ([S]/([S] + [Si])) and (b) the thickness of the P(NaStS) layer, grown from the Si−VBC surface via ATRP, on the polymerization time during the preparation of the Si−VBC-*g*-P(NaStS) surface. The [S]/([S] + [Si]) ratio was determined from the XPS core-level spectral area ratio. ([S] + [Si]) is the sum of the sensitivity factor-corrected S 2p and Si 2p core-level spectral areas in a particular sample.

S 2p and Si 2p core-level spectral areas within the sampling depth of a particular surface), and the polymerization time. Similarly, an approximately linear increase in thickness of the grafted P(NaStS) layer on the Si−VBC surface with the polymerization time is also observed (line b in Figure 4). These results suggest that the surface-initiated ATRP of NaStS was a controlled polymerization process with a "living" character. In addition, it was found that, under similar experimental conditions, the growth rate of the grafted P(PEGMA) layer was comparable to that of the grafted P(NaStS) layer (Table 1).

From the thickness and mass density of the VBC layer on Si−VBC (∼0.3 nm and 1.08 g/cm^3, respectively) and molecular weight of VBC (152.6 g/mol), the surface graft density of the initiator was estimated to be about 1.4 units/nm^2. Since the average cross-sectional area of methacrylate and styrene polymers[5,15] prepared by living radical polymerization is about 2 nm^2, the surface initiator efficiency of the present system is estimated to be about 35%. Thus, for the Si−VBC-*g*-P(NaStS) surface (P(NaStS) thickness ∼7 nm) and the Si−VBC-*g*-P(PEGMA) surface (P(PEGMA) thickness ∼8 nm) from 3 h of ATRP, the degrees of polymerization for the P(NaStS) and P(PEGMA) chains are estimated to be 54 and 46, respectively, based on the surface initiator density of 1.4 units/nm^2, an initiator efficiency of 35%, and P(NaStS) and P(PEGMA) densities[50] of 0.80 and 1.46 g/cm^3, respectively.

3.3. Surface Topography. The changes in topography of the Si−H surface after modification by surface-initiated ATRP were investigated by AFM. Figure 5 shows the representative AFM images of (a) the as-prepared Si−H surface, (b) the Si−VBC surface, (c, d) the Si−VBC-*g*-P(NaStS) surfaces at the respective ATRP time of 3 and 8 h, and (e, f) the Si−VBC-*g*-P(PEGMA) surfaces at the respective ATRP time of 3 and 8 h. The freshly prepared Si−H surface is rather uniform and smooth, with a root-mean-square surface roughness value (R_a) of about 0.18 nm. The Si−VBC surface remains molecularly uniform with a R_a of about 0.25 nm. After surface graft polymerization of NaStS and PEGMA via ATRP for 3 h, the R_a values for the Si−VBC-*g*-P(NaStS) surface and the Si−VBC-*g*-P(PEGMA) surface have increased slightly to about 1.2 and 1.0 nm, respectively. The only slight change in the R_a values indicates that the ATRP-mediated graft polymerization has proceeded uniformly on the VBC-functionalized silicon surface. As shown in Figure 5c,e, the grafted P(NaStS) and P(PEGMA) chains on the modified silicon surface exist as a distinctive overlayer. After the prolonged polymerization time of 8 h, the ATRP-mediated graft polymerization has given rise to a denser coverage of P(NaStS) and P(PEGMA) on the Si−VBC surfaces, as shown in parts d and f of Figure 5, respectively. Molecularly smooth surfaces, with the corresponding R_a values of only about 0.22 and 0.34 nm, were obtained for the two modified silicon substrates. The above results indicate that the surface-initiated polymerizations via ATRP have proceeded uniformly to give rise to dense polymer coverages on the Si−H surfaces.

3.4. Block Copolymer Brushes. One of the unique characteristics of the polymers synthesized by ATRP is the preservation of the active end groups during the polymerization process. Thus, it is possible to synthesize well-defined block copolymers via the ATRP process. To confirm the existence of the "living" chain ends on the Si−VBC-*g*-P(NaStS) surface (or the Si−VBC-*g*-P(PEGMA) surface), surface-initiated ATRP is again used to synthesize the P(NaStS)-*b*-P(PEGMA) (or P(PEGMA)-*b*-P(NaStS)) diblock copolymer brushes from the functionalized silicon surface, using the grafted P(NaStS) (or P(PEGMA)) (Figure 1) as the macroinitiator.

The formation of block copolymer brushes was confirmed by XPS and ellipsometry. The C 1s core-level spectra of the Si−VBC-*g*-P(NaStS) surface from 3 h of ATRP and the corresponding Si−VBC-*g*-P(NaStS)-*b*-P(PEGMA) surface after 3 h of ATRP with PEGMA are shown in parts a and b of Figure 6, respectively. The C 1s core-level spectrum of the Si−VBC-*g*-P(NaStS) surface can be curve-fitted into three peak components having BE's at about 284.6, 285.5, and 286.2 eV, attributable to the *C*−H, *C*−S, and *C*−Cl species, respectively.[37,38] The *C*−S peak components are associated with the P(NaStS). The corresponding C 1s core-level spectrum of the Si−VBC-*g*-P(NaStS)-*b*-PPEGMA surface can be curve-fitted with three peak components with BE's at about 284.6, 286.2, and 288.5 eV, attributable to the *C*−H, *C*−O, and O=*C*−O species, respectively.[37,38] The appearance of the two prominent new peak components, assigned to the *C*−O and O=*C*−O species of PEGMA, confirms that PEGMA has been successfully block copolymerized on the Si−VBC-*g*-P(NaStS) surface. In addition, the C 1s core-level line shape in Figure 6b suggests that the Si−VBC-*g*-P(NaStS)-*b*-P(PEGMA) surface is dominated by the P(PEGMA) blocks. An 8 nm increase in thickness of the grafted P(PEGMA) layer was detected by ellipsometry after the ATRP of PEGMA at 30 °C for 3 h (Table 2). The increase in surface film thickness corresponded to the addition of a P(PEGMA) block with a degree of polymerization of about 46, assuming that the surface density of the P(NaStS) macroinitiator remained the same as that of the initial VBC initiator. The above results confirm that the dormant sites at the end of the grafted P(NaStS) chains allow the reactivation of the graft polymerization process, resulting in the formation of the block copolymer brushes on the functionalized silicon surface. The water contact angle of the as-prepared Si−VBC-*g*-P(NaStS) surface was about 29°.

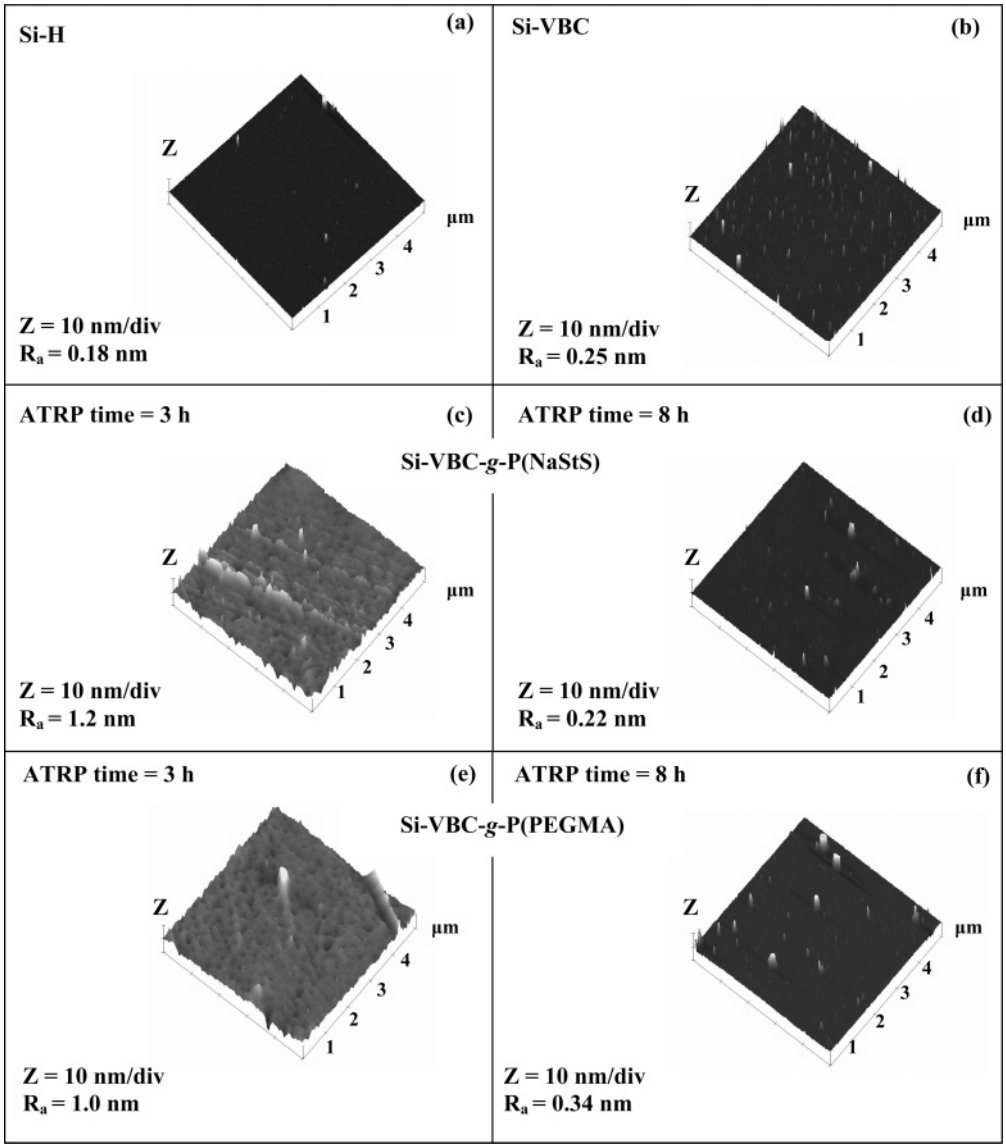

Figure 5. AFM images of (a) the Si−H surface, (b) the Si−VBC surface, (c, d) the Si−VBC-*g*-P(NaStS) surfaces obtained at ATRP time of 3 and 8 h, respectively, and (e, f) the Si−VBC-*g*-P(PEGMA) surfaces obtained at ATRP time of 3 and 8 h, respectively.

Table 2. Static Water Contact Angle, Layer Thickness, and Surface Composition of the Block Graft-polymerized Silicon Surfaces

sample	static water contact angle (±3°)	layer thickness (±1 nm)	surface compositions[a]	
			P(NaStS) (mol %)	P(PEGMA) (mol %)
Si−VBC-*g*-P(NaStS)-*b*-P(PEGMA) surface[b]	44	15	0.0	100
Si−VBC-*g*-P(PEGMA)-*b*-P(NaStS) surface[c]	34	13	71	29

[a] Composition within the sampling depth of the XPS technique (~7.5 nm of the top surface) and determined from the S 2p and O=*C*−O peak component area ratio. [b] The thickness of the starting Si−VBC-*g*-P(PEGMA) surface was about 7 nm; reaction conditions: [PEGMA]:[CuCl]:[$CuCl_2$]:[Bpy] = 100:1:0.2:2, temperature 30 °C for 3 h. [c] The thickness of the starting Si−VBC-*g*-P(PEGMA) surface was about 8 nm; reaction conditions: [NaStS]:[CuCl]:[$CuCl_2$]: [Bpy] = 100:1:0.2:2, temperature 30 °C for 3 h.

However, the water contact angle of the Si−VBC-*g*-P(NaStS)-*b*-P(PEGMA) surface has increased to about 44°, which is comparable to that of the Si−VBC-*g*-P(PEGMA) surface.

Figure 6c,d shows the respective wide scan spectra of the as-prepared Si−VBC-*g*-P(PEGMA) surface from 3 h of ATRP and the corresponding Si−VBC-*g*-P(PEGMA)-*b*-P(NaStS) surface after 3 h of ATRP with NaStS. Comparison of the two wide scan spectra revealed that the Na 1s and S 2p signals have appeared on the Si−VBC-*g*-P(PEGMA)-*b*-P(NaStS) surface. The corresponding Na 1s core-level spectrum (at the BE of about 1068.5 eV)[47] and S 2p core-level spectrum (with the S $2p_{3/2}$ and S $2p_{1/2}$ peak components at the BE's of about 163.8 and 165 eV, respectively)[46] are shown in parts e and f of Figure 6, respectively. The appearance of the Na 1s and S 2p signals confirms the existence of "living" chains on the Si−VBC-*g*-P(PEGMA) surface, and the grafted P(PEGMA) chains can serve as macroinitiators. An approximately 5 nm increase in film thickness was detectd by ellipsometry after the ATRP of NaStS at 30 °C for 3 h on the Si−VBC-*g*-P(PEGMA). The increase in surface film thickness corresponded to the addition of a P(NaStS) block with a degree of polymerization of about 40. The smaller thickness (than the sampling depth of the XPS technique) of the P(NaStS) blocks

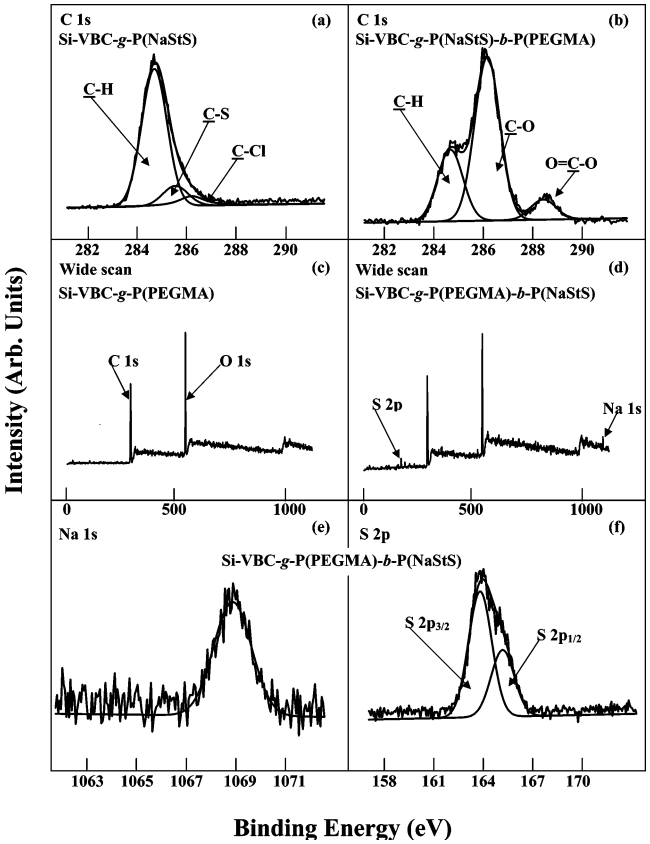

Figure 6. C 1s core-level spectra of (a) the Si−VBC-*g*-P(NaStS) surface obtained at the reaction time of 3 h and (b) the Si−VBC-*g*-P(NaStS)-*b*-PPEGMA surface; wide scan spectra of (c) the Si−VBC-*g*-P(PEGMA) surface obtained at the reaction time of 3 h and (d) the Si−VBC-*g*-P(PEGMA)-*b*-P(NaStS) surface; and (e) Na 1s and (f) S 2p core-level spectra of the Si−VBC-*g*-P(PEGMA)-*b*-P(NaStS) surface. The reaction conditions for the preparation of the Si−VBC-*g*-P(NaStS)-*b*-PPEGMA surface were [PEGMA]:[CuCl]:[$CuCl_2$]:[Bpy] = 100:1:0.2:2, temperature = 30 °C for 3 h, and for the preparation of the Si−VBC-*g*-P(PEGMA)-*b*-P(NaStS) surface were [NaStS]:[CuCl]:[$CuCl_2$]:[Bpy] = 100:1:0.2:2, temperature = 30 °C for 3 h.

allows a portion of the underlying P(PEGMA) blocks to be detected unambiguously by the XPS technique. The compositions of the surface grafted diblock copolymers within the sampling depth of the XPS technique (∼7.5 nm in an organic matrix[49]) are shown in Table 2. Finally, the water contact angle of the Si−VBC-*g*-P(PEGMA)-*b*-P(NaStS) surface decreases to about 34°, from about 43° for the starting Si−VBC-*g*-P(PEGMA) surface.

4. Conclusions

A simple one-step process for the covalent immobilization of an ATRP initiator monolayer on the hydrogen-terminated Si(100) (Si−H) surface was demonstrated. The process involved direct UV-induced coupling of the vinyl group of 4-vinylbenzyl chloride (VBC) with the Si−H surface to give rise to the Si−VBC surface. The process represented a considerable simplification over the multistep processes. Well-defined polymer−Si hybrids, consisting of covalently tethered polymer brushes of NaStS and PEGMA via surface-initiated ATRP on the Si−VBC substrates, could be readily prepared. Kinetic studies revealed an approximately linear increase in graft concentration and thickness of the surface graft-polymerized brushes with the polymerization time, indicating that the chain growth from the functionalized silicon surface was a controlled process. The present surface-initiated ATRP also allowed the preparation of functional polymer−Si hybrids with molecularly flat surfaces. The "living" chain ends on the silicon surface could be used as macroinitiators for further functionalization of the hybrid surfaces via block copolymerization.

References and Notes

(1) Milner, S. T. *Science* **1991**, *251*, 905.
(2) Halperin, A.; Tirrell, M.; Lodge, T. P. *Adv. Polym. Sci.* **1992**, *100*, 31.
(3) Buriak, J. M. *Chem. Rev.* **2002**, *102*, 1272.
(4) Husemann, M.; Morrison, M.; Benoit, D.; Frommer, J.; Mate, C. M.; Hinsberg, W. D.; Hedrick, J. L.; Hawker, C. J. *J. Am. Chem. Soc.* **2000**, *122*, 1844.
(5) Shah, R. R.; Mecerreyes, D.; Husemann, M.; Rees, I.; Abbott, N. L.; Hawker, C. J.; Hedrick, J. L. *Macromolecules* **2000**, *33*, 597.
(6) Kong, X.; Kawai, T.; Abe, J.; Iyoda, T. *Macromolecules* **2001**, *34*, 1837.
(7) Linford, M. R.; Fenter, P.; Eisenberger, P. M.; Chidsey, C. E. D. *J. Am. Chem. Soc.* **1999**, *121*, 11513.
(8) Royea, W. J.; Juang, A.; Lewis, N. S. *Appl. Phys. Lett.* **2000**, *77*, 1988.
(9) Sieval, A. B.; Demirel, A. L.; Nissink, J. W. M.; Linford, M. R.; Van der Maas, J. H.; de Jeu, W. H.; Zuilhof, H.; Sudholter, E. J. R. *Langmuir* **1998**, *14*, 1759.
(10) Letant, S. E.; Sailor, M. J. *Adv. Mater.* **2001**, *13*, 335.
(11) Kato, K.; Uchida, E.; Kang, E. T.; Uyama, Y.; Ikada, Y. *Prog. Polym. Sci.* **2003**, *28*, 209.
(12) Jordan, R.; UIman, A. *J. Am. Chem. Soc.* **1998**, *120*, 243.
(13) Ingall, M. D. K.; Honeyman, C. H.; Mercure, J. V.; Bianconi, P. A.; Kunz, R. R. *J. Am. Chem. Soc.* **1999**, *121*, 3607.
(14) Prucker, O.; Ruehe, J. *Macromolecules* **1998**, *31*, 602.
(15) Husseman, M.; Malmström, E. E.; McNamara, M.; Mate, M.; Mecerreyes, D.; Benoit, D. G.; Hedrick, J. L.; Mansky, P.; Huang, E.; Russell, T. P.; Hawker, C. J. *Macromolecules* **1999**, *32*, 1424.
(16) Baum, M.; Brittain, W. J. *Macromolecules* **2002**, *35*, 610.
(17) Ejaz, M.; Yamamoto, S.; Ohno, K.; Tsujii, Y.; Fukuda, T. *Macromolecules* **1998**, *31*, 5934.
(18) Zhao, B.; Brittain, W. J. *J. Am. Chem. Soc.* **1999**, *121*, 3557.
(19) Yamamoto, S.; Ejaz, M.; Tsujii, Y.; Fukuda, T. *Macromolecules* **2000**, *33*, 5608.
(20) Wang, J. M.; Matayjaszewski, K. *J. Am. Chem. Soc.* **1995**, *117*, 5614.
(21) Matayjaszewski, K.; Patten, T. E.; Xia, J. *J. Am. Chem. Soc.* **1997**, *119*, 674.
(22) Qiu, J.; Matayjaszewski, K. *Macromolecules* **1997**, *30*, 5643.
(23) Davis, K. A.; Paik, H. K.; Matayjaszewski, K. *Macromolecules* **1999**, *32*, 1767.
(24) Wang, J. L.; Grimaud, T.; Matayjaszewski, K. *Macromolecules* **1997**, *30*, 6507.
(25) Coessens, V.; Pintauer, T.; Matayjaszewski, K. *Prog. Polym. Sci.* **2001**, *26*, 337.
(26) Granville, A. M.; Boyes, S. G.; Akgur, B.; Foster, M. D.; Brittain, W. J. *Macromolecules* **2004**, *37*, 2790.
(27) Ejaz, M.; Yamamoto, S.; Tsujii, Y.; Fukuda, T. *Macromolecules* **2002**, *35*, 1412.
(28) Zhao, B.; Brittain, W. J. *Macromolecules* **2000**, *33*, 8813.
(29) Yu, W. H.; Kang, E. T.; Neoh, K. G. *J. Phys. Chem. B* **2003**, *107*, 10198.
(30) Zhao, B.; He, T. *Macromolecules* **2003**, *36*, 8599.
(31) Boyes, S. G.; Brittain, W. J.; Weng, X.; Cheng, Z. D. *Macromolecules* **2002**, *35*, 4960.
(32) Wang, J. Y.; Chen, W.; Liu, A. H.; Lu, G.; Zhang, G.; Zhang, J. H.; Yang, B. *J. Am. Chem. Soc.* **2002**, *124*, 13358.
(33) Ejaz, M.; Ohno, K.; Tsujii, Y.; Fukuda, T. *Macromolecules* **2000**, *33*, 2870.
(34) Branch, D. W.; Wheeler, B. C.; Brewer, G. J.; Leckband, D. E. *Biomaterials* **2001**, *22*, 1035.
(35) Sieval, A. B.; Linke, R.; Zuilhof, H.; Sudhölter, J. R. *Adv. Mater.* **2000**, *12*, 1457.
(36) Boukherroub, R.; Bensebaa, S. M. F.; Wayner, D. D. M. *Langmuir* **1999**, *15*, 3831.
(37) Beamson, G.; Briggs, D. *High-resolution XPS of Organic Polymer: the Scienta ESCA300 Database*; John Wiley: Chichester, UK, 1992; p 278.

(38) Moulder, J. F.; Stickle, W. F.; Sobol, P. E.; Bomben, K. D. In *X-ray Photoelectron Spectroscopy*; Chastain, J., Ed.; Perkin-Elmer: Eden Prairie, MN, 1992; p 43.
(39) Iddon, P. D.; Robinson, K. L.; Armes, S. P. *Polymer* **2004**, *45*, 759.
(40) Chuy, C.; Ding, J. F.; Swanson, E.; Holdcroft, S.; Horsfall, J.; Lovellb, K. V. *J. Electrochem. Soc.* **2003**, *150*, E271.
(41) Okamura, H.; Takatori, Y.; Tsunooka, M.; Shirai, M. *Polymer* **2002**, *43*, 3155.
(42) Wang, P.; Tan, K. L.; Kang, E. T.; Neoh, K. G. *J. Mater. Chem.* **2001**, *11*, 2951.
(43) Zhang, F.; Kang, E. T.; Neoh, K. G.; Huang, W. *J. Biomater. Sci., Polym. Ed.* **2001**, *12*, 515.
(44) Boum, M.; Brittain, W. J. *Macromolecules* **2002**, *35*, 610.
(45) Matyjaszewski, K.; Miller, P. J.; Shukla, N.; Immaraporn, B.; Gelman, A.; Luokala, B. B.; Siclovan, T. M.; Kickelbick, G.; Vallant, T.; Hoffmann, H.; Pakula, T. *Macromolecules* **1999**, *32*, 8716.
(46) Moulder, J. F.; Stickle, W. F.; Sobol, P. E.; Bomben, K. D. In *X-ray Photoelectron Spectroscopy*; Chastain, J., Ed.; Perkin-Elmer: Eden Prairie, MN, 1992; p 60.
(47) Moulder, J. F.; Stickle, W. F.; Sobol, P. E.; Bomben, K. D. In *X-ray Photoelectron Spectroscopy*; Chastain, J., Ed.; Perkin-Elmer: Eden Prairie, MN, 1992; p 50.
(48) Kang, E. T.; Neoh, K. G.; Tan, K. L. In *Handbook of Organic Conductive Molecules and Polymers*; Nalwa, H. S., Ed.; Wiley & Sons: Chichester, UK, 1997; p 121.
(49) Tan, K. L.; Woon, L. L.; Wong, H. K.; Kang, E. T.; Neoh, K. G. *Macromolecules* **1993**, *26*, 2832.
(50) *Aldrich Handbook of Fine Chemicals and Laboratory Equipment*: *2003*−*2004*; Sigma-Aldrich Chem. Co.: Milwaukee, WI, pp 1545 and 1512.

MA049225A